



Multicomponent NAPL Solidification Thermodynamics

CATHERINE A. PETERS*, KRISTINE H. WAMMER and CHRISTOPHER D. KNIGHTES

*Department of Civil and Environmental Engineering, Princeton University, Princeton,
NJ 08544, U.S.A.*

(Received 31 July 1998)

Abstract. Nonaqueous phase liquid (NAPL) contaminants that are chemical mixtures often contain compounds that are solids in their pure states. In the environment, weathering processes cause shifts in multicomponent NAPL composition, thereby enriching the NAPL in the less soluble compounds which may result in their eventual solidification. In this paper, we review the thermodynamic theory governing solid–liquid phase equilibria for the multicomponent NAPLs, and we present experimental observations of such phase equilibria for binary, ternary, and quaternary mixtures of polycyclic aromatic hydrocarbons (PAHs). If the NAPL phase behaves as an ideal solution and if the solid precipitate is pure, then a compound's mole fraction solubility limit in the NAPL phase equals its solid–liquid reference fugacity ratio. This value is a constant at the temperature of the system. If the NAPL phase is a non-ideal solvent or if the solid is a solid solution, prediction of NAPL solidification in the environment is considerably more difficult. Experimental results indicate that for compounds such as naphthalene and acenaphthene, the solid–liquid reference fugacity ratio serves as a good indicator of the solubility limits in the NAPL phase. For phenanthrene, the solids that form when this compound exceeds its solubility limit are solid solutions that consistently include large portions of 2-methylnaphthalene. These results suggest that the independent behavior implied by ideal solubility theory may not be an accurate descriptor of NAPL solidification phenomena for all PAH-containing NAPLs.

Key words: NAPL, solidification, polycyclic aromatic hydrocarbon, PAH, coal tar, multicomponent phase equilibrium, thermodynamics, ideal solution theory.

1. Introduction

Polycyclic aromatic hydrocarbons (PAHs) are important environmental contaminants because they are suspected carcinogens and have been listed as priority pollutants (U.S. EPA, 1993). PAHs often exist in the subsurface environment as complex mixtures in dense nonaqueous phase liquids (NAPLs). These materials are particularly prevalent at the sites of former manufactured gas plants (MGPs), where town gas production resulted in uncontrolled releases of coal tar, an or-

* Author for correspondence: Tel.: 609-258-5645; Fax: 609-258-2799;
E-mail: cap@ceor.princeton.edu

ganic liquid consisting primarily of PAHs (Luthy *et al.*, 1994). PAHs also exist in petroleum-derived NAPL contaminants such as crude oil and diesel fuel.

Despite the similarity in molecular structure of PAHs, the aqueous solubilities of these compounds span several orders of magnitude. When PAH-containing NAPLs are present in the porous medium of an aquifer, the different rates of mass transfer of NAPL constituent compounds to the groundwater result in shifts in NAPL composition. These effects have been described previously where it was demonstrated that NAPL composition dynamics occur over periods of years to decades (Peters *et al.*, 1998; Knightes and Peters, 1996). Similar composition dynamics have been reported for multicomponent NAPLs containing mono-aromatic compounds (Garg *et al.*, 1998). As most PAH compounds are solids in their pure states at ambient temperatures, shifts in NAPL composition may affect the liquid phase stability. As the NAPL becomes depleted of the more soluble compounds, it is enriched with the higher molecular weight, less soluble compounds. These compounds can reach their solubility limits and precipitate out as solids. Liquid phase stability of PAH mixtures has been examined in laboratory systems and the existence of solid coal tars at MGP sites has been reported (Peters *et al.*, 1997). The simulations of NAPL composition dynamics presented by Knightes and Peters (1996) and Peters *et al.* (1998) indicate that the solidification process may take several decades in typical subsurface environments. This is an important process, which currently is not described in most NAPL dissolution and transport models.

As solidification will significantly change NAPL behavior in an aquifer environment, it is important that this process is well understood. Specifically, we need to determine the solubility limits in the NAPL phase and the compositions of resulting solid phases. The objective of this paper is to examine the thermodynamics of PAH–NAPL solidification, with particular focus on simplifying assumptions regarding the ideality of the NAPL and solid phases. An experimental study was conducted involving thermal and compositional analyses to determine solid–liquid phase equilibria for binary, ternary and quaternary mixtures of PAH compounds. The experimental results are presented in phase diagrams and are interpreted in the context of thermodynamic theory governing multicomponent phase equilibria for solid–liquid systems. The relevance of NAPL solidification for environmental systems is discussed through a description of how the presence of solidified NAPL constituents affects aqueous phase concentrations.

2. Thermodynamic Theory

2.1. SOLID–LIQUID PHASE EQUILIBRIA

Thermodynamic theory states that fugacities must be equal for components in phases at equilibrium. For a multicomponent system consisting of a solid in equilibrium with a NAPL, the fugacity equality is written most generally as

$$x_i^S \gamma_i^S f_i^S = x_i^{N^*} \gamma_i^N f_i^L, \quad (1)$$

where γ_i is the activity coefficient of component i in the solid (S) and NAPL (N) phases, and x_i is the mole fraction in each phase. The asterisk on the NAPL phase mole fraction implies that this is the solubility limit. Before solidification occurs, the mole fraction in the NAPL phase will be less than x_i^{N*} .

The remaining terms in Equation (1) are the reference fugacities, f_i , of pure i in the solid (S) and liquid (L) phases. For compounds that are solids in their pure states at the system temperature, f_i^L refers to a hypothetical subcooled liquid state. The ratio of liquid–solid reference fugacities, (f^L/f^S) , quantifies the energy required to convert solid i to liquid i at a given temperature. For a compound that exists as a liquid in its pure state at the system temperature, the reference fugacity ratio is unity. Hildebrand and Scott (1950), and later Prausnitz *et al.* (1986), showed that the liquid–solid reference fugacity ratio can be approximated by

$$\ln \frac{f^L}{f^S} = \frac{\Delta h^f}{RT_m} \left(\frac{T_m}{T} - 1 \right) - \frac{\Delta C_p}{R} \left[\left(\frac{T_m}{T} - 1 \right) - \ln \frac{T_m}{T} \right], \quad (2)$$

where Δh^f is the enthalpy of fusion at the melting temperature T_m , T is the system temperature, R is the universal gas constant, and ΔC_p is the difference in the heat capacities of the liquid and solid. This equation allows computation of the reference fugacity ratio for a particular compound at the system temperature given known values of the thermodynamic properties Δh^f , T_m , and ΔC_p , which are available in references such as Daubert and Danner (1989). As discussed by Mukherji *et al.* (1997), the change in heat capacity term may be neglected with only minor errors. It must be stressed, however, that significant errors result if inaccurate values are used for the enthalpy of fusion. It has become commonplace to assume a constant entropy of fusion for rigid organic molecules for estimation of the enthalpy of fusion using $\Delta h^f = T_m \Delta S^f$. As discussed by Peters *et al.* (1997) this should be avoided unless thermodynamic data are unavailable.

Equation (1) can be rearranged to provide a relationship for the solubility limit of i in the NAPL phase

$$x_i^{N*} = \frac{x_i^S \gamma_i^S}{\gamma_i^N} \left(\frac{f^S}{f^L} \right). \quad (3)$$

This relationship demonstrates that the solubility limit for a given compound is proportional to the solid–liquid reference fugacity ratio through terms that describe the composition of the solid phase and the solution ideality of the solid and liquid phases. In this paper, we define these terms collectively as

$$\text{Nonideality factor} \equiv \frac{x_i^S \gamma_i^S}{\gamma_i^N}.$$

There are two ways that Equation (3) may be simplified. First, if the NAPL serves as an ideal solution for compound i , then the activity coefficient in the NAPL phase is unity, that is $\gamma_i^N \approx 1$. The assumption of ideality in the NAPL phase implies that

the other constituents in the NAPL have similar types of molecular interactions with component i as would molecules in a liquid made up of pure i . Because of the molecular structure similarities of PAHs, this is often considered a reasonable assumption for NAPLs that are mixtures of PAHs, and it has been validated for some PAH mixtures through experimental and theoretical work. In a study of dissolution of PAHs from synthetic NAPLs consisting of nine compounds, Mukherji *et al.* (1997) observed γ_i^N values ranging from 0.8 to 1.2. UNIFAC analysis of very complex PAH mixtures representing field data for coal tar NAPLs predicted γ_i^N values in the same range (Peters *et al.*, 1999). Alkylated compounds, which can constitute 10–20% of a coal tar, are predicted to have slight positive deviations indicating self-association tendencies for these compounds.

Another simplification of Equation (3) results if the solid phase is ideal and each component that precipitates does so by forming a pure solid rather than a solid solution. In this case, $x_i^S \gamma_i^S = 1$. The term ‘pure’ when referring to the solid does not imply that all solids present must be the same compound. For a PAH-containing NAPL in the environment, it is likely that more than one component will reach maximum solubility in the NAPL phase and precipitate out. Rather, the term ‘pure’ in this sense means that the solid consists of a heterogeneous mixture of solid phases, each of which is pure in one of the components, and that no solid solutions are formed. Investigations of binary mixtures of naphthalene and phenanthrene, and phenanthrene and anthracene provide some evidence that these combinations of PAHs do not form solid solutions (Rudolfi, 1909).

If both simplifications are applicable, the mole fraction solubility limit of the component in the NAPL is equal to the solid–liquid reference fugacity ratio,

$$x_i^N = \left(\frac{f^S}{f^L} \right)_i. \quad (4)$$

As this relationship implies independence in the solubility limits of constituent compounds, the validity of Equation (4) is of great interest for use in models to predict multicomponent NAPL behavior in porous media. While the assumption of NAPL phase ideality has been studied for a variety of multicomponent NAPLs, the thermodynamics of solid formation and ideality in the solid phase in PAH mixtures has not been examined.

2.2. IMPLICATIONS FOR AQUEOUS PHASE CONCENTRATIONS

In the environment, we must consider a three-phase system consisting of NAPL, solid and aqueous phases. While three-phase systems were not part of this experimental study, the findings regarding the nonideality factor have implications for predicting equilibrium concentrations in the aqueous phase. In the three-phase system, the fugacity in the aqueous phase equals both the fugacities in the solid and NAPL phases

$$x_i^A \gamma_i^A f_i^L = x_i^{N*} \gamma_i^N f_i^L = x_i^S \gamma_i^S f_i^S, \quad (5)$$

where superscript A denotes the aqueous phase. The activity coefficient in the aqueous phase, γ_i^A , refers to a reference state of pure liquid i . Through rearrangement, these equalities provide relationships for the aqueous phase concentration (expressed as a mole fraction)

$$x_i^A = x_i^{N*} \gamma_i^N \frac{1}{\gamma_i^A}, \quad (6)$$

or

$$x_i^A = x_i^S \gamma_i^S \frac{1}{\gamma_i^A} \left(\frac{f^S}{f^L} \right)_i. \quad (7)$$

As the concentrations in the aqueous phase are dilute, γ_i^A can be approximated by the activity coefficient for i in water in equilibrium with pure solute, γ_i^{A*} (Banerjee, 1984)

$$\gamma_i^{A*} = \frac{1}{x_i^{A*}} \left(\frac{f^S}{f^L} \right)_i, \quad (8)$$

where x_i^{A*} is the pure solute aqueous solubility expressed as a mole fraction. Substituting this expression for γ_i^A in Equation (6) yields

$$x_i^A = x_i^{N*} \gamma_i^N x_i^{A*} \left(\frac{f^L}{f^S} \right)_i. \quad (9)$$

Versions of Equation (9) have been discussed previously in the context of investigations into the solubility of multicomponent NAPLs (Peters and Luthy, 1993; Banerjee, 1984; Burris and MacIntyre, 1985; Mackay *et al.*, 1991; Lane and Loehr, 1992; Lee *et al.*, 1992). This relationship shows the dependence of the aqueous solubility of component i on the mole fraction of i in the NAPL phase. In particular, if the NAPL phase is an ideal solution for i , then x_i^A is proportional to the mole fraction in the NAPL phase through the constant $x_i^{A*} (f^L/f^S)$, which is the subcooled liquid solubility of i . When solid has formed and there are three phases present, then the mole fraction in the NAPL phase is at its maximum value as determined by Equation (3). The implication for the aqueous concentration is seen in Equation (7), rewritten here by substituting for γ_i^A from Equation (8)

$$x_i^A = x_i^S \gamma_i^S x_i^{A*}. \quad (10)$$

This relation elucidates the impact of the presence of a solid phase on the aqueous concentration of a NAPL constituent. If the solid is pure, then the aqueous concentration is simply the pure compound's aqueous solubility. If the solid is not pure, but rather a solid solution, then $x_i^S \gamma_i^S$ is not unity, and the aqueous concentration is likely to be less than the aqueous solubility.

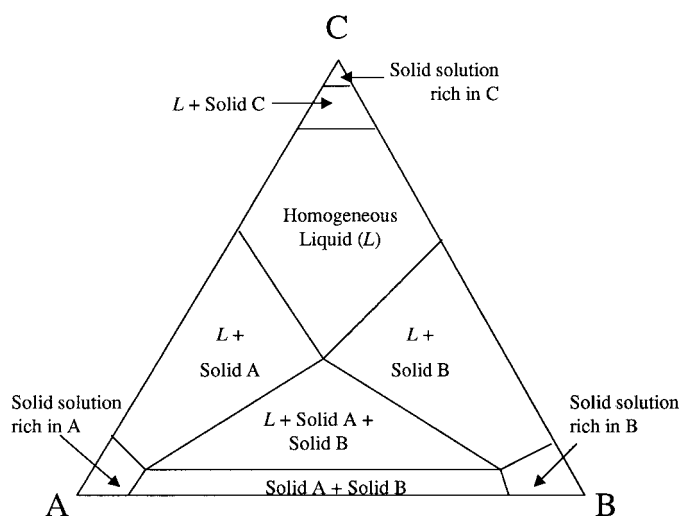


Figure 1. Schematic of general ternary phase diagram (Source: Rhines, 1956).

2.3. ISOTHERMAL PHASE EQUILIBRIUM FOR A TERNARY MIXTURE

Mixtures of PAHs that are solids in their pure states can exist as liquids in certain compositions below the melting temperatures of the constituent compounds, that is PAH mixtures form eutectic systems. For a ternary mixture, this can be depicted with an isothermal ternary phase diagram, which indicates how phase behavior is determined by the overall composition of the mixture at a given temperature. These diagrams are explained in this section. Figure 1 is a hypothetical ternary phase diagram that is representative of the mixtures in this study. A point in the two-dimensional triangular space represents the overall composition of the ternary mixture, where the three axes (perpendicular to the triangle sides) measure the mole fractions of the components. A mixture composition that lies within the L region exists as a homogeneous liquid phase. The boundaries of this region are defined by the solubility limits as given in Equation (3), or, assuming ideality, by Equation (4). Towards the corners of the diagram there exist three single phase regions representing solid solutions that predominantly consist of either A, B or C. These regions of solid solutions are typically small. If the solid is pure, the size of this region is negligible for a given mixture component and the composition of the solid phase is denoted by a point at the triangle corner.

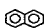
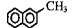

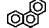
The remaining regions of the ternary diagram consist of multiple phases. Three regions have a liquid phase and a solid phase in equilibrium. In each of these regions only one component of the mixture is in excess of its solubility limit, and the solid phase is a solid solution rich in that component. Between the regions of L and solid solution A and L and solid solution B, is a triangular, three-phase region where both solid solution A and B are present in addition to L. The middle region on the bottom of this diagram consists of two-phase systems with both solid

solutions A and B. In all the regions that pertain to multiple phases, tie lines (not depicted) are used to connect points to indicate the compositions of the liquid and solid phases in equilibrium.

3. Materials and Methods

Solid–liquid phase equilibria were examined for binary, ternary and quaternary mixtures of PAHs, to examine the extent of nonideality in Equation (3). Table I presents molecular structures and thermodynamic properties of the compounds selected for use. These compounds represent a range of types of PAHs. Naphthalene (NPH) and phenanthrene (PHN) are unsubstituted two and three ring PAHs, 2-methylnaphthalene (2MN) is an alkylated PAH, and acenaphthene (ACE) contains a non-aromatic ring structure. Many PAHs have very small solid–liquid reference fugacity ratios (see, e.g., Peters *et al.*, 1997), which means that numerous PAHs may be needed to form a NAPL at ambient temperatures. The alkylated PAH, 2MN, has a large solid–liquid reference fugacity ratio. Its inclusion in this work enables formulation of stable liquid mixtures of only three or four PAHs. Seven groups of PAH mixtures were examined, as indicated in Table II. Binary mixtures were studied at temperatures ranging from the melting points of the pure compounds to the eutectic point for the mixture. Ternary groups were studied at 26°C and 29°C; the quaternary group was studied only at 26°C. These temperatures were selected because they are high enough for formation of liquid mixtures of only a few PAHs, but they are below the melting temperatures of all PAHs in the mixtures. These temperatures are not representative of the cooler temperatures encountered in aquifer environments, but they allow examination of thermal effects which can ultimately be extended to predict behavior at lower temperatures (Equation (2)).

Table I. Properties of the compounds used in experimental systems

	Naphthalene	2-Methylnaphthalene	Acenaphthene	Phenanthrene
Abbreviation	NPH	2MN	ACE	PHN
Structure				
Molecular weight	128	142	154	178
Δh^f [kcal/mol] ^a	4.53	2.89	5.12	3.93
T_m [°C] ^a	80	35	93	99
ΔC_p [kcal/mol K] ^a	2.37	5.72	1.53	3.82
$(f^S/f^L)^b$ at 26°C	0.32	0.87	0.21	0.29
$(f^S/f^L)^b$ at 29°C	0.34	0.92	0.23	0.30

^a Daubert and Danner, 1989.

^b Solid–liquid reference fugacity ratio calculated using Equation (2).

Table II. Experimental systems studied

	Binary	Binary	Binary	Ternary	Ternary	Ternary	Quaternary
NPH	X	–	–	X	–	X	X
2MN	X	X	X	X	X	X	X
ACE	–	X	–	X	X	–	X
PHN	–	–	X	–	X	X	X

3.1. CHEMICALS

Naphthalene at 99+% purity, acenaphthene at 99%, phenanthrene at 98% purity, and 2MN at 98% were obtained from Aldrich Chemical Company (Milwaukee, WI). Optima-grade acetonitrile and methanol were obtained from Fisher Scientific (Pittsburgh, PA). Water was deionized and ultra-purified using HYDRO Picosystem Plus (HYDRO services, RTP, NC). All reagents were used as received. Thermal analysis of the purchased chemicals was done on a Perkin Elmer differential scanning calorimeter (DSC) to verify the literature values of T_m and Δh^f obtained from Daubert and Danner (1989). The measured values did not deviate significantly from the literature values, so the literature values were used unchanged. The liquid–solid heat capacity differences were computed at T_m using correlations in Daubert and Danner (1989).

3.2. BINARY SOLID–LIQUID PHASE EQUILIBRIUM

Solid–liquid phase equilibria were studied for three binary systems using mixtures of 2MN with NPH, ACE or PHN. These experiments were designed to determine the temperature–composition relationships of the phase boundaries between homogeneous liquid systems and two-phase (solid–liquid) systems. For each binary pair, eleven mixtures were studied in batch systems in increments of tenths of mole fraction. Specific compositions were prepared in sealed vials by weighing desired amounts of each compound such that the total mass was about 1 g. Each vial was heated until the contents formed a homogeneous liquid phase, and then cooled to -15°C causing the contents of the vial to fully solidify. The temperature of the phase transition from two-phase system to homogeneous liquid was determined by heating the vial and observing the temperature when the contents of the vial were fully melted. The phase boundary temperatures were not determined by measuring freezing points via cooling because of the tendency of these mixtures to form subcooled liquids. Two similar protocols were followed depending on the phase boundary temperatures: (a) 20°C and up and (b) 8 – 20°C . Accordingly, each vial was placed in (a) a water bath on a heating mantle or (b) an ice and water bath on a heating mantle. The samples were heated slowly (i.e., $<0.2^\circ\text{C}/\text{min}$). Visual observation indicated the temperature at which the sample was completely liquified.

Temperature was measured using a mercury thermometer with readability of $\pm 1^\circ\text{C}$. For each vial, two replicate observations were made with a typical range of 1°C .

3.3. TERNARY AND QUATERNARY SOLID-LIQUID PHASE EQUILIBRIA

The ternary and quaternary experiments were designed to study solid-liquid phase equilibria at specific temperatures for PAH mixtures of three and four compounds. The overall system compositions were chosen so that in each experimental system only one PAH would exceed its solubility limit. That is, in reference to Figure 1, experiments were designed with overall compositions in the two-phase regions pertaining to liquid phase (L) in equilibrium with a single solid phase. The rationale behind this experimental design is that if ideal solubility theory holds for both the solid and liquid phases, then the solids that form in these systems should be nearly pure in the constituent that is present in excess of its solid-liquid reference fugacity ratio. No experiments were conducted in which 2MN exceeded its solubility limit because of the small size of the composition region. The solid-liquid phase boundary for 2MN in a ternary system with NPH and ACE was previously observed (Peters *et al.*, 1997), and was not re-examined in these experiments. The overall mixture composition of each experimental system was selected to be near the solid-liquid phase boundary to provide a large enough liquid-to-solid volume ratio to facilitate sampling of both phases. Several experimental systems were chosen for each ternary combination to span the range of mixture compositions. Six quaternary mixtures were created so that three pairs of experiments were conducted in which either NPH, ACE or PHN was in excess of its ideal solubility limit.

To prepare each experimental system, the desired amounts of PAHs were measured to an approximate total of 7 g, placed in a 10-ml vial, and sealed tightly with a Teflon cap. The vial was heated to 100°C in a water bath to completely melt the PAHs. The liquid was cooled to approximately 50°C and a sample was taken for chemical analysis to verify the overall system composition. The mixture was then cooled in a water bath over several hours to 26°C or 29°C . The cooling was performed at a rate of approximately 8°C per hour. If samples were permitted to cool too quickly, large pockets of liquids were trapped within the solid matrix in some samples. As centrifuging, a natural choice for phase separation, may result in unknown temperature increases, its use was avoided because of the temperature sensitivity of the phase relationships. When solids were formed slowly, they had a uniform structure and appeared distinct from the liquid phase. In some cases solids did not form, presumably due to lack of a nucleation site. In these cases, vials were tapped forcefully and/or quenched in antifreeze, brought back up to approximately 40°C , and slowly cooled to equilibrium at 26°C or 29°C . After cooling, the vials were allowed to settle for two to three days in an environmental chamber with temperature control precision of $\pm 0.1^\circ\text{C}$. The liquid phase was then sampled with a syringe and decanted.

Samples of the solid phase were taken by randomly selecting three pieces from each vial, briefly drying them on absorbent paper, and rinsing in acetonitrile to remove liquid clinging to the surfaces. This procedure minimized the inclusion of liquid phase with solid samples but it did not prevent it. Some of the solids did not form clean crystals that were easily separated from the liquid phases. With these samples there was some possibility that entrapped liquid was included in the solid sample. For each experiment the compositions of the three solid samples were quite similar to each other and were within estimated measurement error.

3.4. HPLC ANALYSIS

All samples were diluted by a factor of 5×10^4 in methanol. The compounds were separated using a Hewlett Packard 1050 high performance liquid chromatograph (HPLC) with a Hewlett Packard reverse phase C18 column (250 mm \times 4 mm, 5 μ m particle size). The HPLC method consisted of a 1.0-ml/min flow rate of a constant 50% acetonitrile/water mobile phase and 2 μ l injection volume. The concentrations were detected using a diode array UV detector (DAD) set at 223 nm for NPH, 220 nm for ACE and 2MN, and 249 nm for PHN. Calibration curves were made for a range of 1–400 mg/l using standard solutions of each compound dissolved in methanol. Mass concentration was converted to molar concentration, which in turn was converted to mole fractions of each compound by summing the total moles of PAHs in the sample. Measurement error was estimated from the calibration regression error and from the propagation of this error through the mole fraction calculation.

4. Results and Discussion

4.1. BINARY SYSTEMS

Melting temperature observations for the binary mixture experiments are shown as circles in the binary phase diagrams in Figure 2. The results for the binary mixtures of ACE and 2MN and of PHN and 2MN were obtained as part of the present study. The results for the binary mixture of NPH and 2MN were published previously (Peters *et al.*, 1997), but are included here to provide a complete picture of all three binary mixtures involving 2MN.

These diagrams indicate the boundaries in the temperature-composition space that separate regions of homogeneous liquids (above) and regions of two-phase solid–liquid or fully solid systems (below). The solid curves in Figure 2 are phase boundaries predicted by the ideal solubility relationship in Equation (4) combined with the temperature-dependent function of $(f^S/f^L)_i$ in Equation (2). In all three binary systems, these curves predict a eutectic point where the ideal solubility curves intersect. The implication of this type of binary solid–liquid phase diagram is that for temperatures below the melting temperatures of both components, there is a window of compositions that will exist as homogeneous liquids. For example

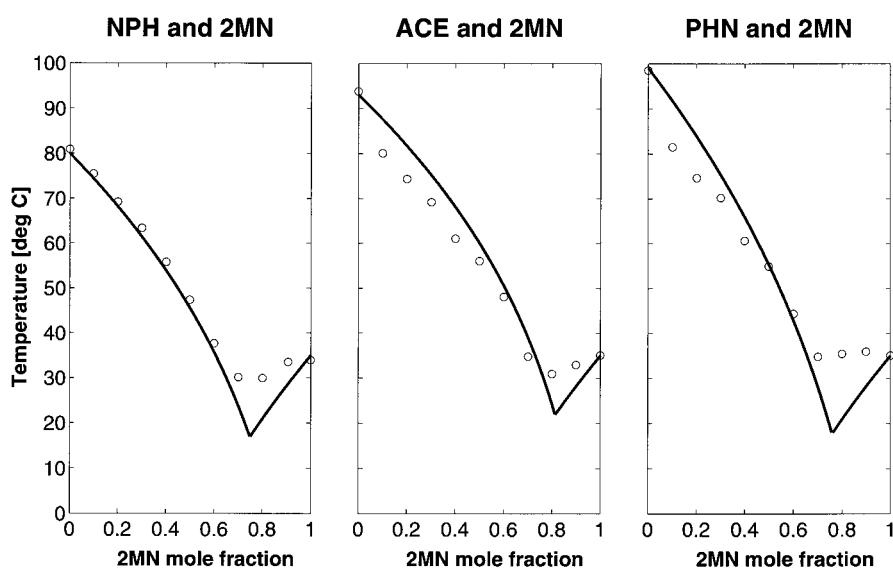


Figure 2. Temperature-composition diagrams of solid-liquid phase equilibria for three binary PAH mixtures. Experimental observations (O) and ideal solubility predictions (—).

at 29°C, ideal solubility theory predicts liquid phase stability for 2MN if its mole fraction is less than 0.92, for NPH if its mole fraction is less than 0.34, for ACE if its mole fraction is less than 0.23, and for PHN if its mole fraction is less than 0.30.

At high temperatures in the two binary systems involving ACE and PHN, the observed phase boundary is below the ideal prediction. At temperatures that are more relevant for environmental systems, the observed phase boundary is above the ideal prediction for all three binary systems. For example, in the NPH/2MN system at 29°C, the liquid phase solubility limit for 2MN is approximately 0.79 (mole fraction) which is significantly less than the ideal prediction of 0.92. This deviation is so significant in the PHN/2MN system that there are no compositions observed to exist as liquids below 35°C even though the eutectic temperature is predicted to be 19°C.

If the observed phase boundary is below the ideal curve, as is the case for ACE and PHN at high temperatures, then the solubility limit is larger than the solid-liquid reference fugacity ratio and the nonideality factor must be greater than unity. As the binary experiments were not designed for chemical analysis of the solid phase, we don't have sufficient information to attribute the deviation to x_i^S or to γ_i^S/γ_i^N . However, because x_i^S cannot exceed 1, in order for the nonideality factor to be greater than unity, γ_i^S/γ_i^N must be greater than unity. If the observed phase boundary is above the ideal curve, as is the case for all three binary mixtures at ambient temperatures, then the nonideality factor must be less than unity. For example, in the NPH/2MN system at 29°C, the solubility limit for 2MN of 0.79 corresponds to a value of $(x_i^S \gamma_i^S/\gamma_i^L)$ for 2MN of 0.86. This may be attributable to

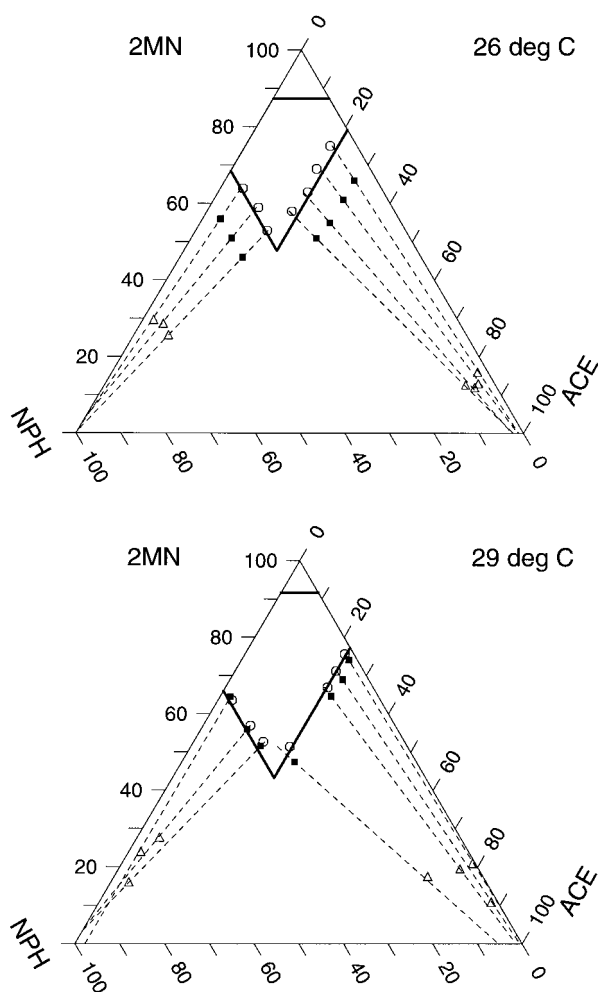


Figure 3. Ternary phase diagrams at 26°C and 29°C of naphthalene, 2-methylnaphthalene, and acenaphthene. Overall system composition (■), liquid (○), solid (△), tie line (- -), ideal solubility prediction (—).

impurity in the solid, in which case $x_i^S \gamma_i^S < 1$, or to nonideality in the liquid phase, or both.

4.2. TERNARY AND QUATERNARY SYSTEMS

The results for the three ternary systems at two different system temperatures, 26°C and 29°C, are presented using ternary phase diagrams in Figures 3–5. Bold solid lines show the ideal solubility limits predicted by mole fraction values equal to the solid–liquid reference fugacity ratios at the system temperatures (Equations (2) and (4)). These lines bound the region of ternary mixture compositions that are pre-

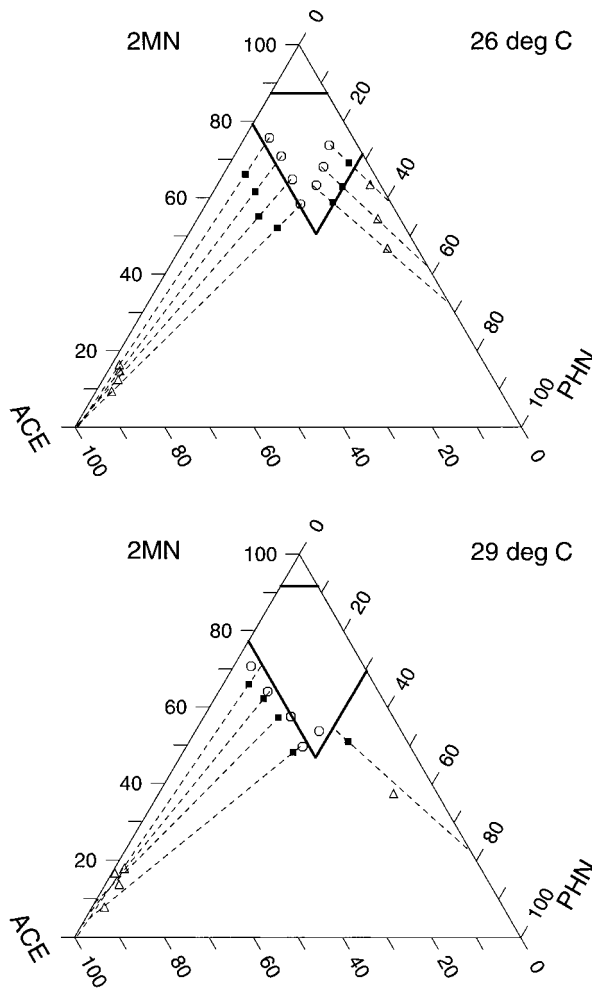


Figure 4. Ternary phase diagrams at 26°C and 29°C of acenaphthene, 2-methylnaphthalene, and phenanthrene. Overall system composition (■), liquid (○), solid (△), tie line (—), ideal solubility prediction (---).

dicted to exist as homogeneous liquids. The effect of the higher system temperature (29°C vs. 26°C) is to increase the size of this stable liquid region.

The solid squares plotted on the ternary phase diagrams indicate the overall system compositions of the ternary experimental systems. Examination of the positions of these points indicates that the experiments were designed to have overall compositions in the two-phase region in which only one of the constituents was in excess of its solubility limit. For experiments in which either NPH or ACE was in excess of solubility, it was possible to conduct experiments in which the overall system composition was near to but in excess of the ideal solubility limit (bold solid line). For PHN, this was sometimes not possible because experiments with such compositions had insufficient liquid phase volume for sampling. When such

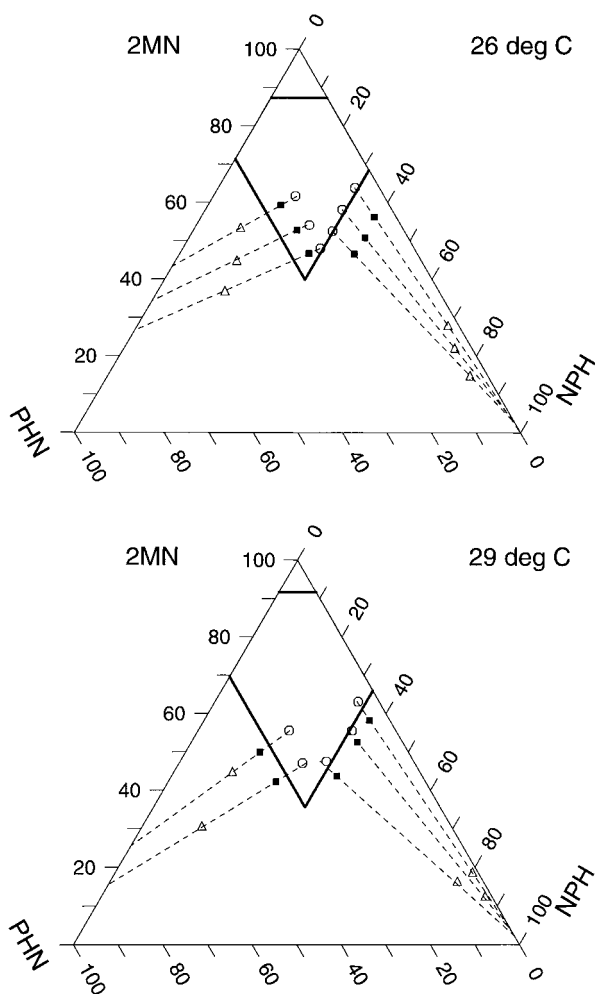


Figure 5. Ternary phase diagrams at 26°C and 29°C of phenanthrene, 2-methylnaphthalene, and naphthalene. Overall system composition (■), liquid (○), solid (△), tie line (- -), ideal solubility prediction (—).

problems occurred, the experimental system was redesigned to have higher PHN content until an overall system composition was obtained in which there was a substantial volume of liquid phase. For some PHN experiments, such as the three in Figure 5(a), the overall composition contained less PHN than the ideal solubility limit. This provided preliminary evidence that for PHN the ideal solubility limit is not the actual solubility limit for these mixtures.

For each experimental system, the measured liquid phase composition is plotted as a circle and the average of the measured solid phase compositions is plotted as a triangle. The estimated standard error in the liquid phase mole fractions is ± 0.02 . The estimated standard error in the solid phase mole fractions ranges from ± 0.01 for less predominant constituents to ± 0.10 for the predominant constituents.

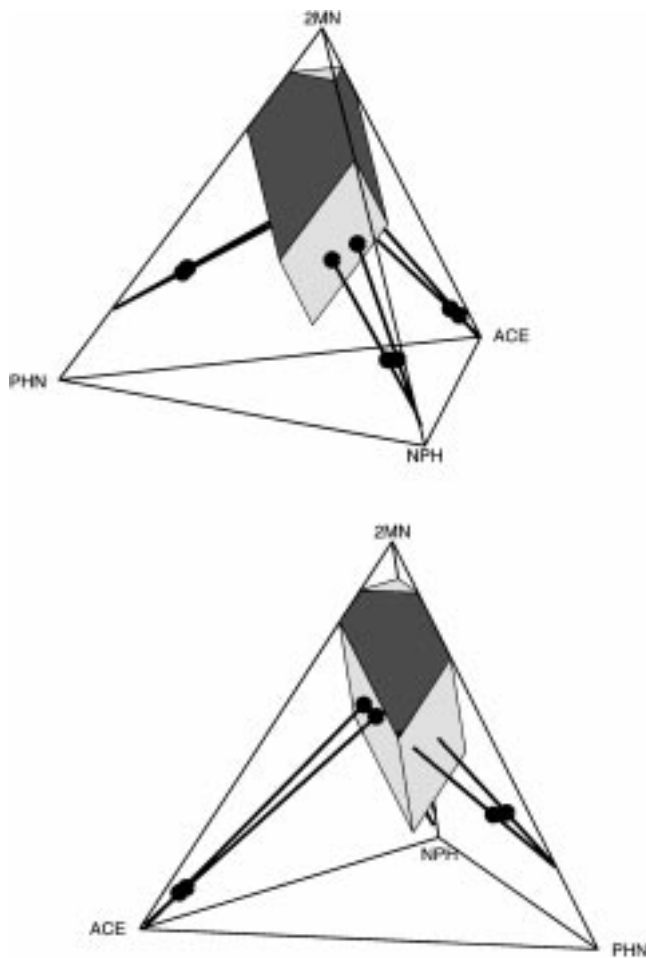


Figure 6. Quaternary phase diagram in two views. Ideal solubility limits are indicated as two-dimensional planar surfaces and experimentally determined tie lines connect observed liquid and solid compositions.

Through a combination of mass balance equations and equations to translate mole fractions to triangular space, it can be shown that the composition of any mixture of the two phases will fall on the tie line connecting the two phase compositions. This is commonly referred to as the ‘lever rule’ in chemical phase equilibria. This means that the overall system composition will fall on the tie line. Hence, each tie line was determined by combining the information from all three composition measurements for that experiment. The dashed tie lines are regressions through the overall composition, the liquid composition and the solid phase composition points. The regression constant parameter was fixed so that the regression line was forced through the overall composition point.

The results for the quaternary system at 26°C are presented in the two views of the tetrahedron in Figure 6. The light gray faces are the planes within the tet-

Table III. Compilation of averages of measured liquid phase solubility limits, estimated solid phase composition with respect to dominant components, and inferred values of the ratio of solid–liquid activity coefficients for all ternary and quaternary experiments

Solubility-limited PAH	Expt'l system	No. of expts. averaged	(f^S/f^L)	Measured x_i^{N*}	By tie line extrapolation χ_i^S	Inferred γ_i^S/γ_i^N
NPH	Ternary 26°C	3	0.32	0.30	0.98	0.98
NPH	Ternary 29°C	3	0.34	0.32	0.97	0.99
NPH	Ternary 26°C	3	0.32	0.31	0.98	1.00
NPH	Ternary 29°C	3	0.34	0.33	0.97	1.00
NPH	Quat. 26°C	2	0.32	0.32	0.95	1.10
ACE	Ternary 26°C	4	0.21	0.19	0.98	0.94
ACE	Ternary 29°C	4	0.23	0.22	0.97	1.02
ACE	Ternary 26°C	4	0.21	0.19	1.00	0.93
ACE	Ternary 29°C	4	0.23	0.24	0.96	1.12
ACE	Quat. 26°C	2	0.21	0.21	0.98	1.03
PHN	Ternary 26°C	3	0.29	0.21	0.56	1.37
PHN	Ternary 29°C	1	0.30	0.28	0.78	1.17
PHN	Ternary 26°C	3	0.29	0.21	0.65	1.11
PHN	Ternary 29°C	2	0.30	0.25	0.79	1.02
PHN	Quat. 26°C	2	0.29	0.25	0.79	1.10

rahedron depicting the mole fraction values of the solid–liquid reference fugacity ratios for each compound. The three-dimensional region within these boundaries represents overall system compositions that are predicted by ideal solubility theory to be homogeneous liquids. As was the case with the ternary experiments, the quaternary experiments were designed to have overall system compositions with only one constituent in excess of its solubility limit. For visual simplicity in the three-dimensional diagram, the overall system compositions were not plotted. For each experimental system, the measured liquid-phase composition is plotted along with the average of the three measurements of the solid-phase composition. A tie line is shown connecting these two points, extending to and ending at the face of the tetrahedron that it intersects.

4.3. LIQUID PHASE BOUNDARIES

Ideal solubility theory predicts that if solid i has formed, then the mole fraction of that constituent in the liquid phase is equal to the solid–liquid reference fugacity ratio (Equation 4). Averages of the measured liquid phase mole fractions of the solubility-limited compounds for all the ternary and quaternary experiments are shown in Table III. In the 18 experiments in which ACE was the compound ex-

ceeding its ideal solubility limit (four ternary systems and the quaternary system) the liquid phase compositions consistently fall on or near the ideal solubility lines (see Figures 3, 4, 6). This implies that ACE behaves ideally in a variety of PAH mixtures and at different temperatures. Similarly, in the 14 experiments in which NPH was the compound exceeding its ideal solubility limit (four ternary systems and the quaternary system) the liquid phase compositions consistently fall on the ideal solubility lines (see Figures 3, 5, 6). That is, the measured values of x_i^{N*} for ACE and NPH are well predicted by (f^S/f^L) at the system temperature.

Very consistent deviant behavior is observed for PHN. In all of the 11 experiments in which PHN was the compound exceeding its ideal solubility limit the liquid phase compositions consistently fall inside the ideal solubility region (see Figures 4, 5, 6). That is, the observed solubility limit for PHN is consistently less than its solid–liquid reference fugacity ratio. This was expected even prior to chemical analysis of the liquid-phase samples given that the overall system compositions for these experiments were also inside the ideal solubility region. These findings imply that the nonideality factor is consistently less than unity for PHN, in a variety of PAH mixtures and at different temperatures.

4.4. SOLID PHASE COMPOSITIONS AND SOLUTION NONIDEALITY

Ideal solubility theory dictates that if solid i has formed then the solid will be pure in that compound. On the phase diagrams, this translates into solid composition points near the corners. For example, in the ternary phase diagrams in Figure 3 the six experiments on the left sides are in excess only of naphthalene's ideal solubility limit. If ideal solubility theory holds, the solid phases would be nearly pure NPH which corresponds to the composition associated with the lower left corner.

The fact that the solid sample observations do not lie in the corners indicates that the solid samples contained some amount of all three PAHs. This indicates that either the solids are true solid solutions, or the solid samples contained some mixture of solid and liquid phases. Because of the difficulty in solid sampling, we cannot rule out the latter. ACE-rich solids formed well-defined crystals that could be separated from the liquid phase relatively cleanly and resulted in high concentrations of ACE in the samples. The NPH- and PHN- rich systems formed a slurry of powdery solid and liquid, or formed waxy solids that may have encapsulated pockets of liquid phase. Despite the difficulty in solid phase sampling, these measurements are still quite informative because they provide information about the slopes of the tie lines in the two-phase regions. Mass balance considerations dictate that overall system compositions lie along the tie line. It follows that the composition of a subsample of this system containing a mixture of the solid and some liquid will also fall along this line. This implies that we can use the three observations for each experimental system to make inferences about the slopes of the tie lines, even though we do not know the exact position of the tie line end

points. For this reason, the tie lines were plotted to extend beyond the solid phase composition points, ending at the intersection with the triangle (or tetrahedron).

Examination of the tie lines in the six ternary phase diagrams and in the quaternary diagram indicates consistent behavior for ACE in that the tie lines all point to the corners. A number of the solid phase composition measurements are very near the corners as well. These results suggest that the solid phases in these systems very likely contain nearly pure ACE, that is $x_i^S \gamma_i^S \cong 1$. This indication of ideal behavior is consistent with the findings of ideal behavior of the ACE liquid phase boundaries. NPH tie lines also consistently point to the corners and some of the solid phase composition measurements are near the corners. This suggests that the solid phases in these experiments are pure NPH. Thus, for ACE and NPH there is considerable evidence that under a variety of temperature and composition conditions the nonideality factor is unity. Furthermore, the individual terms that constitute this factor are approximately unity.

Phenanthrene's tie lines consistently do not point to the corners. We can definitively conclude that in addition to containing PHN, the solids that form in these experiments contain appreciable quantities of 2MN and may also contain some of the third (and fourth) constituents. The finding based on the liquid observations that the nonideality factor for PHN is consistently less than unity could be largely due to the impurity of the solid phase, that is $x_i^S \gamma_i^S < 1$.

By assuming the compositions of the solid phases are near the intersections of the tie lines and the triangle edges/corners, we can gain quantitative information about the nonideality factor. The composition of the solid phase for a given experiment was approximated from the composition indicated by the intersection of the tie line with the triangle (or tetrahedron) boundaries. For ACE and NPH, this is quite a good assumption because there is considerable evidence that the solid phases are nearly pure. For PHN, it is an assumption that impurity in the solid phase is only due to 2MN because all the PHN tie lines intersect the PHN/2MN binary edges. Even in the quaternary experiments, the two PHN tie lines intersect the PHN/2MN edge and not one of the tetrahedron faces. Table III lists the averages of the solid phase mole fractions of the dominant constituent as determined by these tie line intersections. The solid phase is estimated to be nearly pure for ACE and NPH with average x_i^S values ranging from 0.95 to 1.0. The solid phases determined from the PHN tie lines are found to have PHN mole fractions ranging from 0.56 to 0.79, indicating the prevalence of solid solutions.

The combination of the estimated values of x_i^S and the measured values of x_i^{N*} allows inference of the part of the nonideality factor that is the ratio of solid-liquid activity coefficients. Values of γ_i^S/γ_i^N were computed using Equation (3), and are listed in Table III. For NPH, and ACE, values of γ_i^S/γ_i^N are very close to unity, ranging from 0.93 to 1.1. For PHN these values range from 1.0 to 1.37. While the nonideality factor for PHN is made less than unity by $x_i^S < 1$, this effect is offset by the γ_i^S/γ_i^N term being greater than unity. The true magnitude of the γ_i^S/γ_i^N term is uncertain because of the uncertainty in x_i^S , but we can definitely say that γ_i^S/γ_i^N

is greater than unity for PHN. The uncertainty in x_i^S is a bias towards a larger value. The true x_i^S values for PHN are either equal to or less than the values inferred from the tie line intersection points. This implies γ_i^S/γ_i^N values even larger than those reported in Table III. We cannot determine whether the deviation of this term from unity is due to γ_i^S values greater than unity or γ_i^N values less than unity. However, in general, smaller values of x_i^S correlate to larger values of γ_i^S/γ_i^N indicating that the deviation from ideality may be due to the γ_i^S term.

The nonideal behavior results obtained in the binary experiments involving PHN and 2MN can be compared with the observations from the ternary and quaternary experiments involving excess PHN. The binary results indicate that the ideal solubility prediction of the liquid phase region along the PHN–2MN binary edges of the phase diagrams overestimates the size of this window. Indeed, laboratory efforts to generate liquid mixtures of these two compounds in the indicated composition/temperature ranges were unsuccessful. On the ternary phase diagrams, if we connect the points representing the liquid phase compositions for the experiments involving excess PHN, and extrapolate to the PHN–2MN edge, we see a consistent finding with the binary experiments. That is, while ideal solubility theory predicts stable liquid mixtures of PHN and 2MN at ambient temperatures, our experiments indicate that such systems do not form.

5. Summary and Conclusions

Prediction of the environmental behavior of NAPLs containing PAHs must account for the fact that these materials may solidify over time. The thermodynamic relationships for solid–liquid phase equilibria predict that the mole fraction solubility limit of a constituent in the NAPL phase is proportional to the solid–liquid reference fugacity ratio through a collection of terms defined here as the nonideality factor. The nonideality factor is unity if the solid that forms is pure and if the NAPL phase behaves as an ideal solution. In this case, the mole fraction solubility limit equals the solid–liquid reference fugacity ratio which is an easily estimated temperature-dependent constant for a given compound.

Through experimental study of phase equilibrium in binary, ternary and quaternary mixtures, the validity of ideal solubility theory was examined for four PAH compounds. Ideal behavior was observed for ACE and NPH under a variety of composition and temperature conditions. That is, for these compounds, the mole fractions in the liquid phase were found to be well described by the ideal solubility limit, and the solid phases were pure. With an appropriate level of caution, we may extrapolate these findings to complex mixture NAPLs in the environment, and say that the solidification behavior of ACE and NPH can be predicted independent of the composition of the other constituents.

Nonideal behavior was observed for PHN and 2MN. These two compounds are mutually soluble in the solid phase so the solid phase that forms when one of them precipitates is likely to contain appreciable amounts of the other compound. For

systems in which PHN is present in excess of its solubility limit, the solid that forms contains 2MN despite the fact that 2MN has not exceeded its solubility limit. One can think of this as a partitioning process in which 2MN dissolves to some extent in the solid PHN phase. The implication, and the difficulty, is that the solubility limit for PHN is a function of its mole fraction in the solid phase, which is something other than unity. This interdependence significantly complicates the prediction of PHN and 2MN solidification in multicomponent PAH-containing NAPLs.

Acknowledgements

This research was supported by the National Science Foundation under Grant No, EAR 9805376 and by a grant from the U.S. Environmental Protection Agency through the Northeast HSRC to Princeton University (Project #R-69). The authors also acknowledge Dr. George W. Scherer for the use of DSC equipment, and Ms. Emily H. Wood for assistance in sample preparation and analysis. The authors also acknowledge an anonymous reviewer for suggestions that substantially improved the rigor of this presentation.

References

- Banerjee, S.: 1984, Solubility of organic mixtures in water, *Environ. Sci. Tech.* **18**, 587–591.
- Burris, D. R., and MacIntyre, W. G.: 1985, Water solubility behavior of binary hydrocarbon mixtures, *Environ. Toxic. Chem.* **4**, 371–377.
- Daubert, T. E. and Danner, R. P.: 1989, *Physical and Thermodynamic Properties of Pure Chemicals: Data Compilation*, Hemisphere Publishing Co., New York.
- Garg, S., Nie, Y., Rixey, W. G.: 1998, Dissolution of aromatic hydrocarbons from residually trapped hydrocarbon mixtures, In: C. V. Chrysikopoulos, T. C. Harmon and J. Bear (eds) *Proc. 1998 Symp. on Environ. Models and Experiments Envisioning Tomorrow, EnviroMEET'98, Behavior and Remediation of Nonaqueous Phase Contaminants in the Subsurface* Irvine, CA, pp. 91–100.
- Hildebrand, J. H. and Scott, R. L.: 1950, *The Solubility of Nonelectrolyte*, 3rd edn, Reinhold Publishing Co. New York, NY, Ch. 17.
- Knightes, C. D., Peters, C. A.: 1996, Numerical simulation of multicomponent NAPL dissolution and precipitation, *WEFTEC '96, Proc. Water Environment Federation, 69th Annual Conference*, Dallas, TX., Vol. I, Part I: Wastewater Treatment Research, pp. 333–343.
- Lane, W. F. and Loehr, R. C.: 1992, Estimating the equilibrium aqueous concentrations of polynuclear aromatic hydrocarbons in complex mixtures, *Environ. Sci. Tech.* **26**, 983–990.
- Lee, L. S., Hagwall, M., Delfino, J. J. and Rao, P. S. C.: 1992, partitioning of polycyclic aromatic hydrocarbons from diesel fuel into water, *Environ. Sci. Tech.* **26**, 2104–2110.
- Luthy, R. G., Dzombak, D. A., Peters, C. A., Roy, S. B., Ramaswami, A., Nakles, D. V. and Nott, B. R.: 1994, Remediating tar-contaminated soils at manufactured gas plant sites: technological challenges, *Environ. Sci. Tech.* **28**, 266A–276A.
- Mackay, D., Shiu, W. Y., Maijanen, A., and Feenstra, S.: 1991, Dissolution of Nonaqueous phase liquids in groundwater, *J. Contaminant Hydrology* **8**, 23–42.
- Mukherji, S., Peters, C. A., and Weber, W. J. Jr.: 1997, Mass Transfer of Polynuclear Aromatic Hydrocarbons from Complex DNAPL Mixtures, *Environ. Sci. Tech.* **31**, 416–423.
- Peters, C. A. and Luthy, R. G.: 1993, Coal tar dissolution in water-miscible solvents: experimental evaluation, *Environ. Sci. Tech.* **27**, 2831–2843.

- Peters, C. A., Mukherji, S., Knightes, C. D. and Weber, W. J. Jr.: 1997, Phase stability of multicomponent NAPLs containing PAHs, *Environ. Sci. Tech.* **31**, 2540–2546.
- Peters, C. A., Blackburn, E. D., and Celia, M. A.: 1998, Spatial and temporal variation of composition in multicomponent NAPLs, In: V. N. Burganos, G. P. Karatza, A. C. Payatakes, C. A. Brebbia, W. G. Gray and G. F. Pinder (eds), *Proc. XII Int. Conf. Comput. Meth. Water Resour. Comput. Mech. Publ.*.
- Peters, C. A., Mukherji, S., Weber, W. J. Jr.: 1999, UNIFAC modeling of multicomponent NAPs containing polycyclic aromatic hydrocarbons, *Environ. Toxicology and Chem.* **18**(3).
- Prausnitz, J. M., Lichtenthaler, R. N., de Azevedo, E. G.: 1986, *Molecular Thermodynamics of Fluid Phase Equilibria*, 2nd edn, Prentice-Hall: Englewood Cliffs, New Jersey, Ch. 9.
- Rhines, F. N.: 1956, *Phase Diagrams in Metallurgy, Their Development and Application*, McGraw Hill: New York, Ch. 14.
- Rudolfi, E.: 1909, *Zeitschrift für physikalische Chemie*, **66**, 705–732.
- US EPA: 1993, Provisional Guidance for Quantitative Risk Assessment of Polycyclic Aromatic Hydrocarbons, Office of Research and Development, United States Environmental Protection Agency, Washington, DC. EPA/600/R-93/089.